Coherent reflection of He atom beams from rough surfaces at near-grazing incidence

Bum Suk Zhao, H. Christian Schewe, Gerard Meijer, and Wieland Schöllkopf*
Fritz-Haber-Institut der Max-Planck-Gesellschaft, Faradayweg 4-6, 14195 Berlin, Germany
(Dated: May 21, 2010)

We here report coherent reflection of thermal He atom beams from various microscopically rough surfaces at grazing incidence. For a sufficiently small normal component k_z of the incident wave-vector of the atom the reflection probability is found to be a function of k_z only. This behavior is explained by quantum-reflection at the attractive branch of the Casimir-van der Waals interaction potential. For larger values of k_z the overall reflection probability decreases rapidly and is found to also depend on the parallel component k_x of the wave-vector. The material specific k_x dependence for this classical reflection at the repulsive branch of the potential is explained qualitatively in terms of the averaging-out of the surface roughness under grazing incidence conditions.

PACS numbers: 34.35.+a, 03.75.Be, 68.49.Bc

Coherent reflection of an atom from a solid surface can happen via two different mechanisms; quantum or classical reflection. In *quantum reflection* an atom is reflected at the long-range attractive part of the atom-surface potential [1], whereas an atom is classically reflected at the turning point of the potential's repulsive branch. Recently, quantum reflection from solid surfaces has been observed with ultracold metastable Ne [2] and He atoms [3], with a Bose-Einstein condensate [4], and with ^{3}He [5] and ^{4}He [6] atom beams of thermal energies. In these experimental studies classical reflection at the repulsive branch of the potential was considered to be negligible, either because of deexcitation of the metastable atoms [2, 3], inelastic scattering or adsorption [4], or surface roughness [5]. Quantum reflection was also theoretically studied, using the long-range Casimir-van der Waals atom-surface potential, indicating that the reflection probability is only a function of k_z, the component of the incident wave-vector that is perpendicular to the surface [1].

Classical reflection of atom beams from solid surfaces has been studied intensively for decades, see e.g. [7]. In most of those investigations, however, clean crystalline surfaces that are smooth at the atomic level and that have been kept clean under ultra-high vacuum conditions have been used. In addition, scattering of He atoms from disordered surfaces has been used to investigate local perturbations of the surface including ad-atoms, steps, clusters, etc. [8–10]. For microscopically rough surfaces it was generally accepted that atoms would not be coherently reflected, but would undergo diffuse scattering. The reflection of atom beams from rough surfaces was investigated in a few experiments only [11, 12]. More recently, microscopic surface roughness has been investigated in the context of the Casimir force between macroscopic bodies (see e.g. Refs. [13–15]) as well as the Casimir-Polder interaction between an atom and a rough [16] or a corrugated surface [17].

In this article we report on coherent reflection of He atom beams from rough surfaces. We present reflection probabilities of He atom beams grazing various planar surfaces: (i) a glass slide for optical microscopy; (ii) a GaAs wafer; (iii) a chromium surface; and (iv) a 20-μm-period chromium grating. Even though details of the reflection probability depend on the material and character of the surfaces, a general behavior is found for each surface when the incident wave-vector of the He atom beam is varied. At small k_z the reflection probability is observed to depend only on k_z, whereas at larger k_z the reflection probability also depends on the wave vector component parallel to the surface; the larger the parallel wave vector component is, the larger is the reflectivity for a given value of k_z. We attribute the behavior at low k_z to quantum reflection as described recently [6], while the behavior at larger k_z is rationalized in terms of a classical-reflection model.

The measurements were done with an apparatus described earlier [6]. The continuous atom beam is formed in a supersonic expansion of He gas at stagnation temperature T_0 and pressure P_0 through a 5-μm-diameter

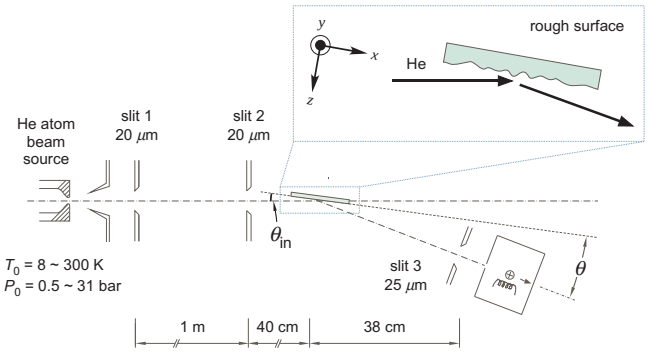

FIG. 1: (Color online) Scheme of the experimental setup. Angular patterns are recorded by scanning the detection angle θ which is defined with respect to the surface plane. In the inset the chosen coordinate system is defined; the xz-plane and the z-axis are the plane of incidence and the surface normal, respectively, while the y-axis is parallel to the detector pivot axis.

orifice into high vacuum. After passing a skimmer of 500 μm diameter, the beam is collimated by two 20-μm-wide slits (S1 and S2) separated by 100 cm as indicated in Fig. 1. In combination with the 25-μm-wide detector-entrance slit (S3), located 78 cm downstream from the second slit, the angular width of the atom beam is 130 μrad FWHM (full width at half maximum). The third slit and the detector (an electron-impact ionization mass spectrometer) are mounted on a frame which is rotated precisely as indicated in Fig. 1. The surface under investigation is positioned such that the (vertical) detector pivot axis is parallel to the surface and passes through its center. The grazing incidence angle $\theta_{\rm in}$ and the detection angle θ are measured with respect to the surface plane. The reflected beam profiles are obtained by rotating the detector, namely varying θ, and measuring the He signal at each angle.

The glass slide is a simple standard microscope slide (ISO Norm 8037/I). It is made out of soda lime glass, is 1 mm thick, and has a surface area of 76×26 mm^2. It is mounted such that its shorter direction is parallel to the pivot axis. The commercial GaAs wafer is cut along the (100) direction and is 50 mm in diameter. The surface is presumably contaminated with an oxygen layer and slightly doped with Boron. The 20-μm-period chromium grating is the same one used in a previous diffraction experiment [6]. Finally, a flat chromium surface of 100×30 mm^2 area is used for comparison with the grating surface. Both chromium surfaces are made from commercially available chromium lithography blanks.

No in-situ surface preparation such as Ar-ion sputtering or high temperature annealing was applied. As the ambient vacuum is about 5×10^{-7} mbar we expect each surface to be covered to some extent with adsorbate molecules from the background gas. Also, all surfaces were exposed to air for at least several days before mounting them in the vacuum chamber. Therefore we expect the surfaces to be oxidized or oxygen covered. Still, for grazing incidence of the He atom beam intense specular reflection peaks are observed for each surface.

Measurements were made for three stagnation temperatures $T_0 = 300$, 50, and 8.7 K corresponding to incidence wave-vectors k of 112, 46, and 18 nm^{-1}, respectively. To maintain a high atom flux and narrow velocity distribution in the beam and to avoid cluster formation the stagnation pressure P_0 was adjusted to $P_0 = 31$, 26, and 0.5 bar, respectively. Under these conditions the relative total incident He signals as observed without a surface in the beam path are $5.0 : 5.5 : 1.0$, for $T_0 = 300$, 50, and 8.7 K, respectively.

Fig. 2 shows angular profiles of the He atom beam reflected from the microscopy slide at various incidence angles for the three stagnation conditions. In each series the reflected peak height decreases by orders of magnitude as the incidence angle is increased. In addition, broad pedestals that get larger as the incidence angle decreases

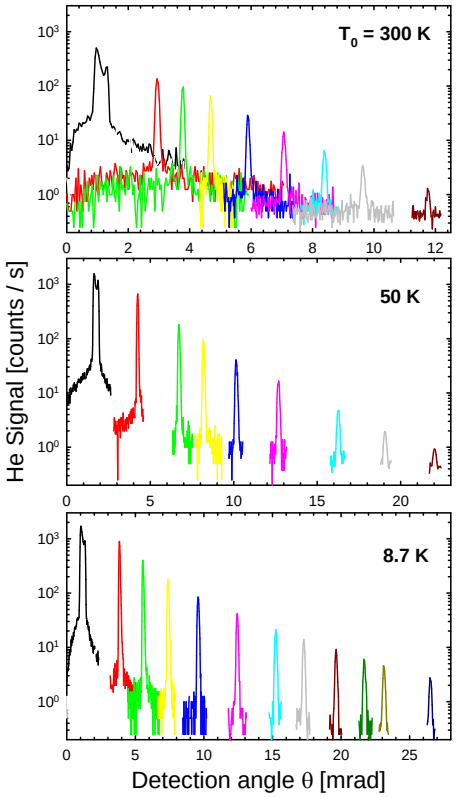

FIG. 2: (Color online) Angular profiles of He atom beams reflected from the microscope slide for (a) $T_0 = 300$ K, (b) 50 K, and (c) 8.7 K. In each measurement the incidence angle $\theta_{\rm in}$ is identical to the detection angle θ at peak center.

are observed under the narrow peaks. We attribute the broad pedestals to incoherent diffuse scattering in contrast to the main peaks which are reflected coherently as evidenced by the observation of diffraction patterns [6]. A double peak structure along with a significant broadening of the main peaks appears for $\theta_{\rm in} \leq 1$ mrad. We tentatively attribute the former to near-field diffraction at the second slit, while the broadening is due to a slight curvature of the glass slide.

The reflection probabilities are determined from the integrated intensity of the reflected peak normalized to the peak area of the incident beam. To determine the reflection probability of the grating surface the sum of all diffraction-peak areas is normalized to the peak area of the incident beam and multiplied by two, thereby accounting for the 50% chromium coverage of the grating surface [6]. To allow for comparison between different source conditions the reflection probabilities are plotted in Fig. 3 as a function of $k_z = k \sin\theta_{\rm in}$. For the glass slide (Fig. 3(a)), when k_z is smaller than about 0.3 nm^{-1}, the reflection probability is a function of k_z only, and independent of the magnitude of the wave-vector k. In this small-k_z regime the reflection probability decreases steeply from 22% at $k_z = 0.02$ nm^{-1} to about 0.2% at $k_z = 0.3$ nm^{-1}. For k_z larger than 0.3 nm^{-1}, the reflec-

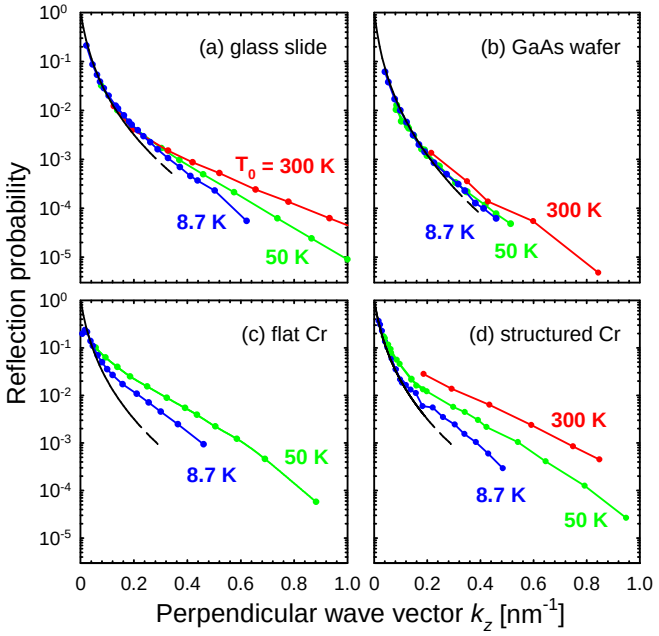

FIG. 3: (Color online) Reflection probabilities for He atom beams at source temperatures of 300, 50, and 8 K for different surfaces: (a) glass slide, (b) GaAs wafer, (c) flat Cr, and (d) microstructured Cr surface. The black lines are fits by a quantum reflection calculation. The colored lines connecting the data points just serve as a guide to the eye.

tion probability curves for different stagnation temperatures T_0, i.e., different incidence wave-vectors k, start to fan out. In this regime, for a given k_z, the observed reflection probability appears to increase with increasing parallel wave-vector component k_x.

The steep decrease at small k_z is explained well by quantum reflection at the attractive branch of the atom-surface interaction potential [6], known as the Casimir-van der Waals potential, approximated by $V(z) = -C_3 l/[(z+l)z^3]$ [1]. Here, C_3 is the van der Waals coefficient, z denotes the distance between the atom and the surface, and l is a characteristic length that is proportional to the transition wavelength between the electronic ground state and the first excited state of the atom (l = 9.3 nm for He). The black lines in Fig. 3 are quantum reflection probabilities obtained by numerically solving the 1-dimensional Schrödinger equation for the attractive potential $V(z)$ with C_3 being the only fit parameter. For the glass slide the best fit to the steep decrease at small k_z is found for a C_3 value of 3×10^{-50} Jm^3.

The reflection probabilities of the GaAs wafer, the flat chromium surface and the periodic chromium surface are plotted in Fig. 3(b)-(d). The black lines in Fig. 3(b)-(d) represent quantum reflection calculations with C_3 = 5, 3, and 3 $\times 10^{-50}$ Jm^3, respectively. The observed reflection probabilities agree well with the quantum reflection model until $k_z \simeq 0.2$ nm^{-1} for the GaAs wafer and $k_z \simeq 0.05$ nm^{-1} for the chromium surfaces. Beyond these values, the observed reflection probabilities start to deviate from the quantum reflection probabilities and to spread out for the different stagnation temperatures. The degree of this fanning out varies for the different surfaces: It is smallest for the GaAs wafer; larger for the glass slide; and the largest for both chromium surfaces. It is noteworthy that this trend coincides with the hierarchy of surface roughness determined independently by qualitative AFM measurements. These measurements indicate the largest root-mean-square surface roughness for the chromium surfaces and the smallest one for GaAs with the glass slide in between.

The combination of a single parameter dependence at small k_z and a fanning out at larger k_z is a general feature for all surfaces we have used in reflectivity measurements. To explain this observation we attribute the behavior at larger k_z to reflection from the repulsive branch of the atom-surface potential, which we refer to as classical reflection to emphasize the contrast to quantum reflection at small k_z.

In the following a qualitative explanation of the increase of classical reflectivity with increasing k_x for a given k_z is described. Atom scattering from a rough repulsive surface potential can be understood as averaged diffraction patterns from the multitude of spatial frequencies within the Fourier spectrum of the rough surface [18]. The (non-specular) diffraction peaks are averaged out leading to a diffusive background signal that does not contribute to the total reflectivity as this is determined from the specular peak intensity only. Therefore, the larger the specular fraction (defined as the ratio of the specular peak intensity to the sum of all peak intensities) is, the higher is the reflectivity. To get an idea of how the specular fraction depends on k_z and k_x for He atoms scattering from one of our surfaces, we have analyzed the diffraction patterns observed with the chromium grating used in Fig. 3(d) [6]. In Fig. 4 the specular fraction is plotted against k_z for the three source conditions.

When k_z is large, the specular fraction stays between 0.5 and 0.6 and is similar for the different $k_x \simeq k$. As k_z decreases for a given k_x, the specular fraction starts to increase at a certain threshold value and approaches unity at $k_z = 0$ nm^{-1}. The vertical lines in Fig. 4 mark the critical values $k_z^* = \sqrt{4\pi k/d}$ at which the negative first order peak disappears for a given k [6], where d is the grating period. Apparently, the observed increase of the specular fraction coincides with the disappearance of the negative first order peak. For k_z smaller than the largest critical value we find a regime where, for a given k_z, the specular fraction increases with k_x. This dependence of the specular fraction on k_x ends at the smallest k_z (less than about $k_z \simeq 0.05$ nm^{-1}), where the curves converge again approaching unity.

The specular fraction approaching unity corresponds to a suppression of the diffraction peaks. This suppres-

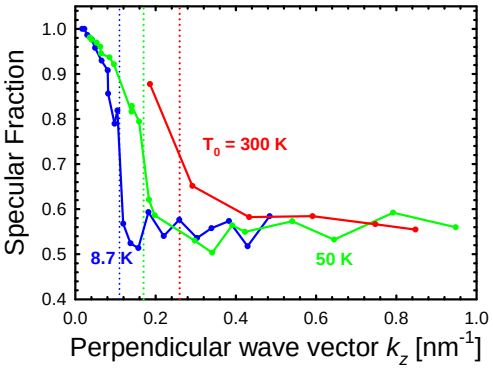

FIG. 4: (Color online) Ratio of specular peak intensity to the sum of all diffraction peak intensities observed with the microstructured Cr surface. The dashed vertical lines mark the critical values k_z^* at which the negative-first-order diffraction peaks appear.

sion was discussed previously for diffraction of atoms from a soft corrugated potential at grazing incidence [19]. The physical picture is that at near grazing incidence many periods of a soft potential are probed by the atom during its bounce from the surface. This results in an averaging out of the pase shifts along the various paths thereby effectively suppressing the diffraction effect. This phase averaging effect is expected to increase with decreasing angle and, hence, with increasing k_x for given k_z just as it is found in the data shown in Fig. 4.

Within this picture it is conceivable that, qualitatively, the same specular fraction behavior, exemplified here by a 20 μm periodic length, would be found for any single spatial-frequency component of the rough surface spectrum. The relevant k_z scale, however, will vary because the critical values k_z^* depends on the periodic length d; for a short periodic length component, the behavior described above occurs at large k_z, while it happens at small k_z for a long periodic length component. Hence, averaging the specular fraction over a range of periodic lengths for a given k_z is qualitatively equivalent to averaging the curves of Fig. 4 over a range of k_z. This results in a larger specular fraction and, hence, larger reflectivity of a rough surface with increasing k_x at given k_z.

In summary, we observed coherent reflection of thermal He atom beams from microscopically rough surfaces of glass, GaAs, and Cr. For small k_z the reflection probability is found to be a universal function of k_z that is modeled well by quantum reflection [6]. For larger k_z the reflection probability is found to increase with k_x for a given k_z. The latter behavior has been discussed qualitatively in terms of an effective averaging-out of the surface roughness. For a quantitative analysis an improved theoretical model will be needed accounting for the actual potential between an atom and a rough surface which could be obtained by extending the theory for the periodically corrugated surface [20, 21] to the randomly rough surface.

B.S.Z. acknowledges support by the Alexander von Humboldt Foundation and by the Korea Research Foundation Grant funded by the Korean Government (KRF-2005-214-C00188). We thank Markus Heyde for help with the AFM measurements, Stephan Schulz for supplying the chromium surfaces, and Samuel A. Meek for support with the computer code.

* Electronic address: wschoell@fhi-berlin.mpg.de

[1] H. Friedrich, G. Jacoby, and C. G. Meister, Phys. Rev. A **65**, 032902 (2002).
[2] F. Shimizu, Phys. Rev. Lett. **86**, 987 (2001).
[3] H. Oberst, Y. Tashiro, K. Shimizu, and F. Shimizu, Phys. Rev. A **71**, 052901 (2005).
[4] T. A. Pasquini et al., Phys. Rev. Lett. **93**, 223201 (2004).
[5] V. Druzhinina and M. DeKieviet, Phys. Rev. Lett. **91**, 193202 (2003).
[6] B. S. Zhao, S. A. Schulz, S. A. Meek, G. Meijer, and W. Schöllkopf, Phys. Rev. A **78**, 010902(R) (2008).
[7] E. Hulpke, G. Benedek, V. Celli, and G. Comsa, eds., *Helium atom scattering from surfaces* (Springer, Berlin, 1992).
[8] R. B. Gerber, Chem. Rev. **87**, 29 (1987).
[9] B. Poelsema and G. Comsa, eds., *Scattering of thermal energy atoms from disordered surfaces*, vol. 115 of *Springer tracts in modern physics* (Springer, Berlin, 1989).
[10] D. Farías and K. H. Rieder, Rep. Prog. Phys. **61**, 1575 (1998).
[11] D. R. O'Keefe and R. L. Palmer, J. Vac. Sci. Technol. **8**, 27 (1971).
[12] B. F. Mason and B. R. Williams, Surf. Sci. **180**, L134 (1987).
[13] G. L. Klimchitskaya, A. Roy, U. Mohideen, and V. M. Mostepanenko, Phys. Rev. A **60**, 3487 (1999).
[14] P. A. Maia Neto, A. Lambrecht, and S. Reynaud, Phys. Rev. A **72**, 012115 (2005).
[15] P. J. van Zwol, G. Palasantzas, and J. Th. M. De Hosson, Phys. Rev. B **77**, 075412 (2008).
[16] V. B. Bezerra, G. L. Klimchitskaya, and C. Romero, Phys. Rev. A **61**, 022115 (2000).
[17] B. Döbrich, M. DeKieviet, and H. Gies, Phys. Rev. D **78**, 125022 (2008).
[18] C. Henkel, K. Mølmer, R. Kaiser, N. Vansteenkiste, C. I. Westbrook, and A. Aspect, Phys. Rev. A **55**, 1160 (1997).
[19] C. Henkel, H. Wallis, N. Westbrook, C. I. Westbrook, A. Aspect, K. Sengstock, and W. Ertmer, Appl. Phys. B **69**, 277 (1999).
[20] E. Kirsten and K. Rieder, Surf. Sci. **222**, L837 (1989).
[21] D. A. R. Dalvit, P. A. Maia Neto, A. Lambrecht, and S. Reynaud, J. Phys. A **41**, 164028 (2008).